Korean J. Chem. Eng., 37(8), 1436-1439 (2020)
DOI: 10.1007/s11814-020-0578-2

pISSN: 0256-1115
eISSN: 1975-7220

Ultra-fast fabrication of anode-supported solid oxide fuel cells via microwave-assisted sintering technology

Kyeong Joon Kim*, Jeong Hwa Park*, and Kang Taek Lee,†**

*Department of Energy Science and Engineering, DGIST, Daegu 42988, Korea
**Department of Mechanical Engineering, KAIST, Daejeon 34141, Korea
(*Received 1 April 2020 • Revised 29 April 2020 • Accepted 11 May 2020*)

Abstract−We demonstrate ultra-fast fabrication of anode-supported solid oxide fuel cells (SOFCs) using microwave-assisted sintering technology. Due to the nature of microwaves that transfers heat directly into the material, the SOFC sintering process was completed within 8 h, ~ six times faster compared to a conventional sintering process (~47 h). Despite extremely rapid processing time, the microstructure of the SOFC fabricated by microwave-assisted sintering (M-SOFC) was almost identical to that of the conventionally sintered SOFC. Moreover, the electrochemical performance of the M-SOFC at 750 °C was 0.52 W/cm^2 in peak power density, which is even higher than that of the conventionally sintered sample (0.49 W/cm^2). Thus, our results demonstrate that the ultra-fast microwave-assisted sintering process is a highly effective and practically promising technology for fabricating high performance SOFCs.

Keywords: Solid Oxide Fuel Cells, Microwave-assisted Sintering, Anode Support, Ultra-fast Fabrication, Electrochemical Performance

INTRODUCTION

Solid oxide fuel cells (SOFCs) have been recognized as attractive and efficient devices for electrochemical energy conversion [1,2]. SOFCs operating at high temperatures are attracting more attention due to fuel flexibility, high efficiency, and low pollutant emission [3,4]. To reduce the ohmic resistance and improve the electrochemical performance of the SOFC system, SOFCs based on anode-support structures with thin electrolytes (<10 μm) have been intensively investigated [5-7]. However, in the conventional sintering process, the fabrication of anode-supported SOFC using a thin-film electrolyte takes a long processing time (including heating, cooling, and duration) due to multiple sintering steps at different sintering temperatures. For example, before coating of a thin-film electrolyte layer, an anode substrate is pre-sintered at 900 °C for several hours, and then the anode/electrolyte multilayer structure is typically sintered at ~1,400 °C for another several hours [8,9]. In addition, a cathode layer screen-printed on the sintered electrolyte is fired in the temperature range of 1,000-1,200 °C for 2 h [10-12]. However, to prevent the ceramic multilayers of an SOFC from cracking or delamination by thermal shock, the use of conventional furnaces requires very slow heating and cooling rates of each step. Thus, the total process time takes tens of hours, resulting in increase of the manufacturing cost [7,13]. To overcome this issue, alternative sintering processes using the microwave have been attempted [14, 15]. In general, the microwave directly interacts with ceramic particulates of samples and thereby provides rapid volumetric heating, resulting in significant reduction in processing time and energy [16]. In microwave-assisted sintering, the energy absorbed by a dielectric material per volume (p) is estimated as Eq. (1) [17]:

$$p = \frac{1}{2}\varepsilon_0 \varepsilon'' \omega E^2 V \quad (1)$$

where E is the electrical field strength, ε_0 is the dielectric constant in a vacuum, ε'' is the dielectric loss factor of the material, ω is the angular frequency of the external electromagnetic field, and V is the material volume. Recently, studies using microwave sintering process for rapid SOFC fabrication have been reported [17-19]. Fujitsu et al. reported that the density of partially stabilized zirconia for 16 minutes in microwave oven was 5.7 g/cm^3, which was similar to density of the conventionally sintered sample at 1,300 °C for 4 h [17]. Gondolini et al. reported that the ionic conductivity of microwave sintered nanocrystalline gadolinium-doped ceria was comparable to conventionally prepared samples [20]. In addition, Jiao et al. fabricated anode support SOFCs with yttria-stabilized zirconia (YSZ) electrolyte by one-step microwave sintering. In that study, the microwave-sintered SOFC exhibited 0.28 W-cm^{-2} in the maximum power density (MPD) at 800 °C [19]. However, the performance of SOFCs fabricated by the microwave-assisted sintering was still lower than that of conventionally processed SOFCs.

In this study, we prepared an anode-supported SOFC by a multi-step microwave sintering process (referred to as M-SOFC). The microstructure of the M-SOFC was investigated by scanning electron microscopy (SEM). The electrochemical performance of M-SOFC was assessed by current-voltage (I-V) characteristics and electrochemical impedance spectroscopy (EIS). Consequently, direct comparison of M-SOFC and conventionally-sintered SOFC (referred to as C-SOFC) demonstrated the effectiveness of the microwave-

†To whom correspondence should be addressed.
E-mail: leekt@kaist.ac.kr

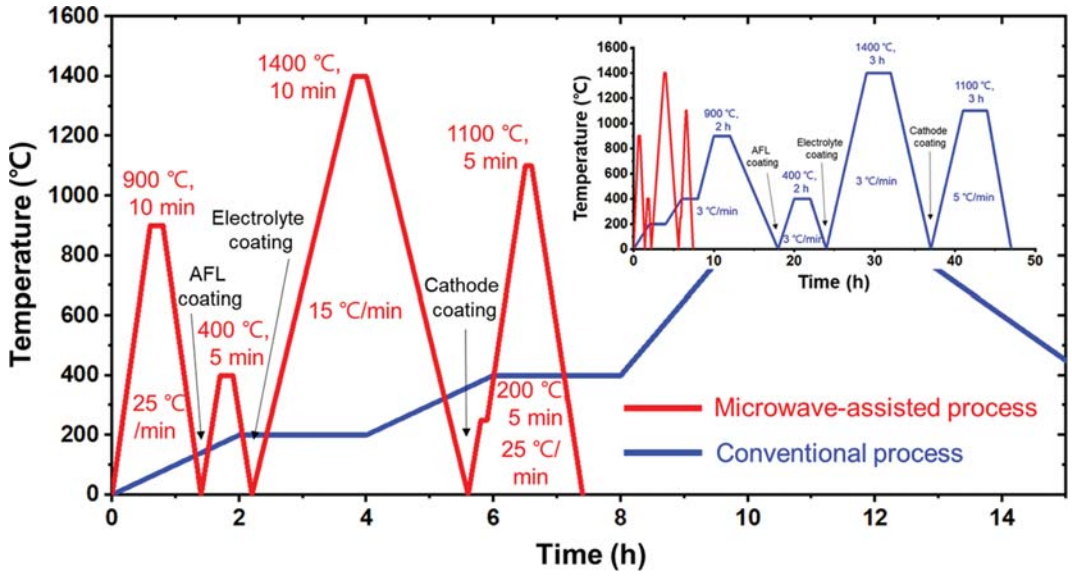

Fig. 1. Sintering schedule of microwave-assisted process. Inset is the conventional process.

assisted sintering process for SOFC fabrication.

EXPERIMENTAL

1. Fuel Cell Fabrication

SOFCs having a structure of NiO-yttria stabilized zirconia (YSZ) anode | NiO-YSZ anode functional layer (AFL) | YSZ electrolyte | LSM-YSZ cathodes were prepared. For NiO-YSZ anode support, a mixture of 65 wt% NiO (Alfa Aesar) and 35 wt% YSZ (TOSOH) in an organic solvent and the binder system was tape-cast and laminated as described in our previous work [7]. For microwave-assisted sintering, a microwave furnace (UMF-04, Unicera, Korea) was used, containing dense SiC as a susceptor to absorb and concentrate the microwaves (2.45 GHz) with power output of 2 kW. For microwave sintering, laminated green anode supports were pre-sintered at 900 °C for 10 min (heating and cooling rate: 25 °C/min). Subsequently, an AFL (60 : 40%) composed of submicron-sized NiO (JT Baker) and YSZ (TOSOH) was deposited on the surface of the pre-sintered body at 400 °C for 5 min (heating and cooling rate: 25 °C/min). After AFL sintering, the YSZ electrolyte suspension was sequentially coated on the anode support by slurry coating and then sintered at 1,400 °C for 10 min (heating and cooling rate: 25 °C/min). The LSM-YSZ cathode with an active area of 1 cm^2 was applied to the YSZ electrolyte layer by blade coating and sintered at 1,100 °C for 5 min (heating and cooling rate: 25 °C/min).

2. Characterization

The microstructure of the SOFC was analyzed using SEM (Hitachi, S-4800). For electrochemical performance measurement, button-type SOFCs were loaded into a fuel cell testing apparatus. The edge of each SOFC on the alumina tube was sealed with Ceramabond 517 (Aremco) to be gastight. The I-V characteristics of the samples were evaluated by a potentiostat (Bio-Logic, VMP-300) at 750 °C with 200 sccm of wet hydrogen (3% of H_2O) at the anode side and dry air at the cathode side. The EIS was measured under the open circuit condition (OCV) over a frequency range from 1 MHz to 0.1 Hz with AC voltage amplitude of 50 mV.

RESULTS AND DISCUSSION

1 Microwave-assisted Sintering Process

Fig. 1 shows the sintering schedule for the microwave sintering process. For comparison purposes, the conventional thermal sintering process was superimposed. Previously, Jiao et al. manufactured anode-supported SOFCs by one-step microwave sintering (at 1,350 °C for 2 h). However, their SOFCs repeatedly showed microcracks in electrolytes and interfaces, probably due to the rapid and simple process. Thus, in this study, we designed a multi-step microwave-assisted process that is similar to conventional sintering steps, as shown in Fig. 1. Therefore, each coated layer (AFL, electrolyte, cathode) was sequentially microwave-sintered at specific temperature to avoid incomplete status (e.g., cracking, warpage, and delamination) at the interface. As a result, the total sintering (including heating and cooling) time of the microwave-assisted process was 7.4 h, which was >6 times faster than that of conventional sintering (47 h).

2. Microstructure of M-SOFC

Fig. 2(a) and 2(b) show the photos of the top view of the C-SOFC and M-SOFC, respectively. Despite the difference in sintering method and time, there is no difference in apparent appearance between the two samples. Fig. 2(c)-(f) shows the localized and magnified top view images by SEM of both samples to compare final microstructures of the YSZ electrolyte and the LSM-YSZ cathode after different sintering processes. The YSZ electrolyte surface of M-SOFC has smaller closed pores and similar grain size compared to that of C-SOFC, indicating that the microwave-assisted sintering even for much shorter duration time at high temperature (10 min at 1,400 °C) is quite effective to densify the solid electrolyte compared to conventional sintering for much longer time process at the same temperature (360 min at 1,400 °C) (Fig. 2(c), (d)). Fig. 2(e) and 2(f) show the LSM-YSZ cathode morphologies of M-SOFC, and C-SOFC,

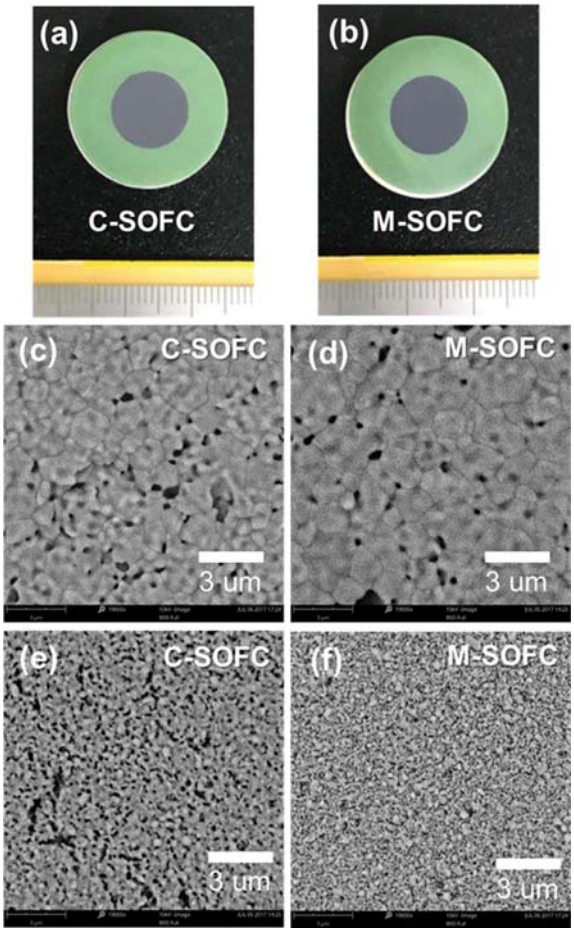

Fig. 2. Photos of the top view of the (a) C-SOFC and (b) the M-SOFC. The magnified top view images of (c) C-SOFC electrolyte, (d) M-SOFC electrolyte, (e) C-SOFC cathode, and (f) M-SOFC cathode.

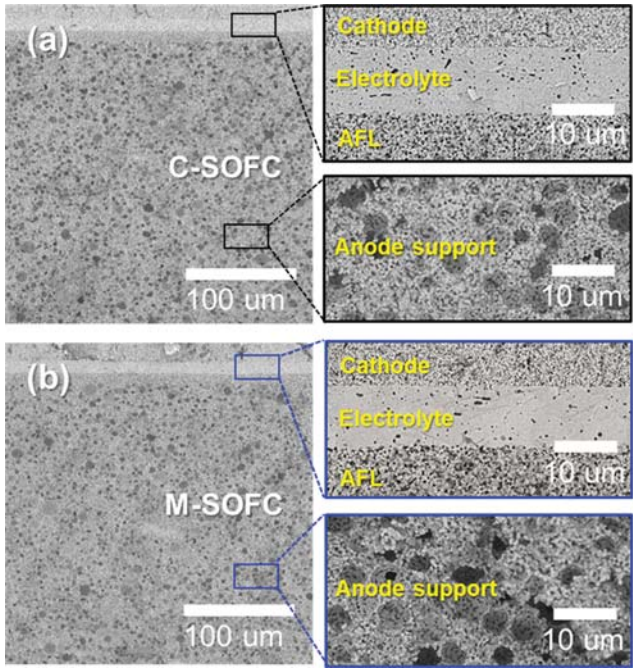

Fig. 3. Cross-sectional SEM images of (a) C-SOFC and (b) M-SOFC. Insets are the magnification view of components for each samples.

respectively. Both cathodes of the M-SOFC and C-SOFC had appropriate porosity. However, the LSM-YSZ cathode of the M-SOFC showed a smaller size of the particulate and pore with homogeneously distributed microstructure compared to that of the C-SOFC. This result suggests that, due to the rapid heating and cooling rates, the microwave sintering process allows the composite electrode to have nanostructures with high porosity, providing more active sites for oxygen reduction reaction for SOFC applications [21].

Fig. 3(a) and 3(b) compare the cross-sectional microstructures of C-SOFC and M-SOFC, respectively, showing that the cathode, electrolyte (~12 μm), AFL, and anode support layers were almost identical for both samples. From the inset image of Fig. 3(b), it is clear that the interface of the multilayer structure of M-SOFC ad-

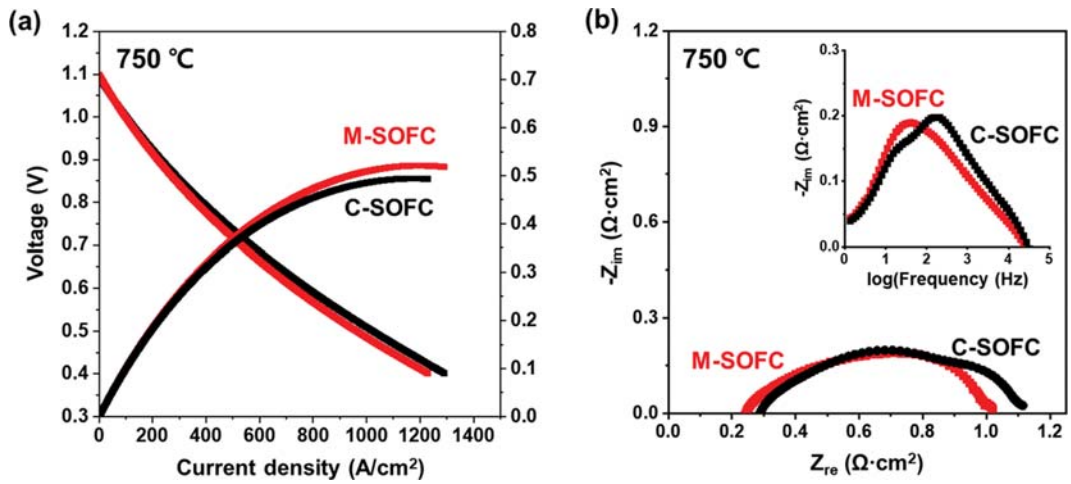

Fig. 4. (a) Current-voltage (I-V-P) characteristics and (b) electrochemical impedance spectra of the M-SOFC and C-SOFC at 750 °C. Inset are the Bode plots.

hered well to each other without delamination even after ultra-fast sintering at rapid heating and cooling rates.

3. Electrochemical Performance of M-SOFC

Fig. 4(a) shows the I-V-P characteristics of the M-SOFC at 750 °C. For comparison purposes, the performance of the C-SOFC was also measured at the same condition and overlapping in Fig. 4(a). The OCV of the M-SOFC was 1.09 V, close to the theoretical value of 1.10 V derived by the Nernst equation, indicating a highly dense electrolyte as well as gastight sealing. The MPD of the M-SOFC was 0.52 W/cm^2, which is comparable to, and even slightly higher, that of C-SOFC (0.49 W/cm^2). To the best of our knowledge, this result is the highest performance among all microwave-assisted SOFCs with YSZ electrolyte [18,19,21,22]. For example, Jiao et al. reported that a similar structured SOFC fabricated by microwave sintering process exhibited less than 0.20 W cm^{-2} in MPD at 750 °C, which is 61% lower than that of our M-SOFC (0.52 W cm^{-2} at 750 °C) [22].

Fig. 4(b) shows Nyquist plots and bode plots (inset) of both samples. From the Nyquist plots, the total (R_t), and ohmic (R_Ω) resistances were calculated from the low and high frequency intercepts at the real axis, respectively. The (non-ohmic) electrode polarization resistance (R_p) was estimated from the difference between the R_t and R_Ω. The calculated R_Ω value for the M-SOFC was 0.24 Ω cm^2 at 750 °C, which is slightly lower R_Ω than that of M-SOFC (0.28 Ω cm^2 at 750 °C). The calculated electrode polarization resistances of M-SOFC and C-SOFC were almost same as 1.02 and 1.10 Ω cm^2, within 8% difference, respectively. Except for the frequencies in the middle range (10^1-10^3 Hz), which is dominant for oxygen surface exchange kinetics of electrode [23,24], the bode plots of both samples show almost identical shapes as a function of frequency. This similar electrochemical performance of the two SOFCs demonstrated that the ultra-fast sintering process using microwaves successfully produced the proper bulk and interface structures of the SOFC for high performance, which is in good agreement with the microstructure observation in Fig. 2 and Fig. 3.

CONCLUSION

We successfully prepared the multilayered structure of the anode supported SOFC with thin YSZ electrolyte via ultra-fast sintering process using microwave-based technology. Total processing time of the microwave-assisted sintering was only 7.4 h, which is ~6 times faster than that of the conventional process. Moreover, SEM analysis revealed that, despite the extremely rapid heating and cooling rates as well as short duration time, the M-SOFC showed a dense electrolyte and uniform and nanostructured electrode, which is desirable for SOFCs to achieve high performance. The electrochemical performance of M-SOFC exhibited 0.52 W/cm^2 in MPD at 750 °C, which is a record-high performance among the YSZ electrolyte-based SOFCs fabricated by the microwave-assisted process. Consequently, these results demonstrated that the cost-effective, energy saving, and ultra-fast microwave-assisted fabrication process is highly feasible for SOFC applications.

ACKNOWLEDGEMENT

This work was supported by the National Research Foundation of Korea (NRF) grant funded by the Korea government (MSIT; The Ministry of Science and ICT) (No. NRF-2020R1A2C2010690, NRF-2019M3E6A1103944).

REFERENCES

1. E. D. Wachsman and K. T. Lee, *Science*, **334**(6058), 935 (2011).
2. K. T. Lee, H. S. Yoon and E. D. Wachsman, *J. Mater. Res.*, **27**(16), 2063 (2012).
3. J.-h. Myung, D. Neagu, D. N. Miller and J. T. Irvine, *Nature*, **537** (7621), 528 (2016).
4. E. D. Wachsman, C. A. Marlowe and K. T. Lee, *Energy Environ. Sci.*, **5**(2), 5498 (2012).
5. B. C. Steele and A. Heinzel, *Nature*, **414**, 345 (2001).
6. D. W. Joh, J. H. Park, D. Kim, E. D. Wachsman and K. T. Lee, *ACS Appl. Mater. Interfaces*, **9**(10), 8443 (2017).
7. J. H. Park, K. T. Bae, K. J. Kim, D. W. Joh, D. Kim, J.-H. Myung and K. T. Lee, *Ceram. Int.*, **45**(9), 12154 (2019).
8. J. Kim, J. Ahn, J. Shin, K. J. Yoon, J.-W. Son, J.-H. Lee, D. Shin, H.-W. Lee and H.-I. Ji, *J. Mater. Chem. A*, **7**(16), 9958 (2019).
9. Y. Zhang, X. Huang, Z. Lu, Z. Liu, X. Ge, J. Xu, X. Xin, X. Sha and W. Su, *J. Am. Ceram. Soc.*, **89**(7), 2304 (2006).
10. D. E. Fowler, A. C. Messner, E. C. Miller, B. W. Slone, S. A. Barnett and K. R. Poeppelmeier, *Chem. Mater.*, **27**(10), 3683 (2015).
11. I. Thaheem, D. W. Joh, T. Noh and K. T. Lee, *Int. J. Hydrogen Energy*, **44**(8), 4293 (2019).
12. D. Kim, J. W. Park, B.-H. Yun, J. H. Park and K. T. Lee, *ACS Appl. Mater. Interfaces*, **11**(35), 31786 (2019).
13. K. J. Kim, M. K. Rath, H. H. Kwak, H. J. Kim, J. W. Han, S.-T. Hong and K. T. Lee, *ACS Catal.*, **9**(2), 1172 (2019).
14. T. Balaji, R. Govindaiah, M. Sharma, Y. Purushotham, A. Kumar and T. Prakash, *Mater. Lett.*, **56**(4), 560 (2002).
15. R. Camaratta, A. C. Lima, M. Reyes, M. Hernandez-Fenollosa, J. O. Messana and C. Bergmann, *Mater. Res. Bull.*, **48**(4), 1569 (2013).
16. Z. Xie, J. Yang, X. Huang and Y. Huang, *J. Eur. Ceram. Soc.*, **19**(3), 381 (1999).
17. S. Fujitsu, M. Ikegami and T. Hayashi, *J. Am. Ceram. Soc.*, **83**(8), 2085 (2000).
18. Z. Jiao, N. Shikazono and N. Kasagi, *J. Power Sources*, **196**(13), 5490 (2011).
19. Z. Jiao, N. Shikazono and N. Kasagi, *J. Power Sources*, **195**(24), 8019 (2010).
20. A. Gondolini, E. Mercadelli, A. Sanson, S. Albonetti, L. Doubova and S. Boldrini, *Ceram. Int.*, **37**(4), 1423 (2011).
21. M. Seyednezhad, A. Rajabi, A. Muchtar and M. R. Somalu, *Ceram. Int.*, **41**(4), 5663 (2015).
22. Z. Jiao, N. Shikazono and N. Kasagi, *J. Power Sources*, **195**(1), 151 (2010).
23. A. Leonide, V. Sonn, A. Weber and E. Ivers-Tiffée, *J. Electrochem. Soc.*, **155**(1), B36 (2007).
24. P. Gansor, K. Sabolsky, J. W. Zondlo and E. M. Sabolsky, *Mater. Lett.*, **105**, 80 (2013).